UDK 669.721.5:620.193
Original scientific article/Izvirni znanstveni članek

ISSN 1580-2949
Mater. Tehnol.

EFFECT OF Sn ON CORROSION PROPERTIES OF HOMOGENIZED Mg-6Zn-0.25Ca MAGNESIUM ALLOY

VPLIV KOSITRA NA KOROZIJSKE LASTNOSTI HOMOGENIZIRANE MAGNEZIJEVE ZLITINE VRSTE Mg-6Zn-0,25Ca

Yingtao Hu[1], Zheng Jia[1,2*], Ronghui Kou[1], Zihui Zhai[1], Xiaowei Niu[2]

[1]School of Mechanical Engineering, Shenyang University, Shenyang 110044
[2]College of Environment, Liaoning Province Pollution Environmental Remediation Professional Technology Innovation Center & Shenyang Key Laboratory of Collaborative Technology Innovation for Industrial Pollution Reduction and Carbon Reduction, Shenyang University, Shenyang 110044, China

Prejem rokopisa – received: 2024-10-28; sprejem za objavo – accepted for publication: 2025-01-29

doi:10.17222/mit.2024.1335

Effect of Sn on the corrosion properties of a homogenized Mg-6Zn-0.25Ca alloy was investigated. The corrosion resistance of ZX60 and ZXT601 alloys was analyzed using XRD, metallography, SEM, mass loss, hydrogen evolution, electrochemical polarization curve and impedance spectrum. The results indicate that Mg-6Zn-Sn-0.25Ca alloy is mainly composed of CaMgSn and $MgZn_2$ phases. After an addition of Sn, the grains are significantly refined, and the volume fraction of the second phase with disperse distribution increases. $MgZn_2$ phase precipitates as well. The addition of Sn can significantly improve the corrosion resistance of Mg-6Zn-0.25Ca alloy, which is mainly due to the smaller grain size, as well as uniformly and densely distributed CaMgSn phase of ZXT601 alloy. Therefore, the passive film formed in the corrosion process is more uniform. The corrosion resistance of ZXT601 alloy is much higher than that of ZX60 alloy.

Keywords: Mg-Zn alloy, homogenization, CaMgSn phase, corrosion properties

Avtorji v članku opisujejo raziskavo vpliva kositra (Sn) na korozijske lastnosti homognenizirane magnezijeve zlitine vrste Mg-6Zn-0,25Ca. Odpornost zlitin proti koroziji tipa ZX60 in ZXT601 so avtorji analizirali s pomočjo rentgenske difrakcije (XRD), vrstične elektronske mikroskopije (SEM), meritev prirastek/izgubo na masi, razvoja dušika, krivulj elektro-kemijske polarizacije in impedančnega spektra. Rezultati analiz so pokazali da je zlitina Mg-6Zn-Sn-0,25Ca v glavnem sestavljena iz faz CaMgSn in $MgZn_2$. Po dodatku (dolegiranju) kositra je prišlo do pomembne rafinacije oziroma zmanjšanja velikosti kristalnih zrn in povečal se je velikostni delež porazdelitve sekundarne faze. Prav tako se je to zgodilo tudi pri fazi $MgZn_2$. Dodatek Sn lahko pomembno izboljša odpornost zlitine Mg-6Zn-0.25Ca proti koroziji, kar je v glavnem posledica udrobljenja kristalnih zrn, enakomerne velikostne porazdelitve CaMgSn faze pri zlitini tipa ZXT601. Zato je tudi pasivni film, ki nastane med procesom korozije bolj enakomerne debeline in enovit po preseku. Odpornost zlitine ZXT601 proti koroziji je precej boljša, kot jo ima zlitina ZX60.

Ključne besede: zlitine na osnovi Mg-Zn, homogenizacija, CaMgSn faza, korozijske lastnosti

1 INTRODUCTION

With the advancement of production technology and cost reduction, magnesium alloys have shown significant application advantages and broad prospects as structural materials in important fields such as aerospace, national defense and military, rail transportation, electronic communication, and biomedicine in recent years. They are known as "the 21st century green engineering materials". In the field of aerospace, magnesium alloys are widely used to manufacture important components for aircraft, missiles, spacecraft, and satellites to significantly reduce the weight of the parts, improve the maneuverability of aircraft, and reduce the launch costs of spacecraft. In the civilian field, the application of magnesium alloys in electronic products has developed rapidly in recent years, and the thin and light laptop casings produced are highly favored. At the same time, China has a broad range of magnesium ores and is the country with the richest magnesium resource reserves in the world, accounting for more than 50 % of the world's total magnesium resources. China is also a major manufacturer of magnesium alloys, and more than 80 % of its magnesium alloy products are exported to the international market. Therefore, we urgently have to determine how to adapt to local conditions, rationally utilize the advantages of magnesium resources in China, accelerate the design, research and development of high-performance magnesium alloys, promote the engineering applications of magnesium alloys, and effectively achieve material lightweighting.

In recent years, low-alloy Mg-Zn-Ca based alloys have received widespread attention due to their excellent room temperature formability, age hardening ability, and biocompatibility.[1–3] In addition, it is difficult to form a dense protective oxide film on the surface of a low-alloy

*Corresponding author's e-mail:
jz140@163.com (Zheng Jia)

ZX alloy due to a lack of passivating elements and a low concentration of solvable alloying elements in the matrix.[4,5] In addition, a coarse $Ca_2Mg_6Zn_3$ cathode phase or Mg_2Ca anode phase is usually formed in a ZX alloy, which is likely to cause local pitting corrosion and damage the corrosion resistance of the alloy.[6,7] Therefore, low strength and poor corrosion resistance have become bottleneck problems, hindering a widespread application of ZX-series low-alloy magnesium alloy.

The standard electrode potential of Sn is –0.13 V, higher than that of Mg, which is –2.37 V.[8] Therefore, adding Sn can increase the surface potential of the magnesium matrix, promote the reduction of the potential difference between the cathode second phase and the magnesium matrix, while inhibiting micro-galvanic corrosion. In addition, Sn has a high solid solubility in magnesium and a significant precipitation strengthening effect. Adding a small amount of Sn can form a high-melting-point Mg_2Sn phase in magnesium and its alloys.[9] Therefore, the role of Sn in magnesium alloys has been studied by researchers at home and abroad. Suresh[10] analyzed the influence of Sn and Ca content on the phase structure of as-cast Mg-Sn-Ca magnesium alloys. The results showed that a mass ratio of Sn to Ca of 2.5 helped to form Mg_2Ca phase at grain boundaries and CaMgSn phase in the matrix. When the mass ratio of Sn to Ca was 3, CaMgSn phase was mainly formed in the magnesium matrix. The Sn element can also improve the corrosion resistance of magnesium and its alloys. For example, when 0.5 % Sn is added to AZ91, the corrosion rate of the alloy is reduced by 18.2 %. This greatly promotes the application of the alloying element Sn in magnesium.[11] Zhao et al.[12] reported that the corrosion resistance of Mg-xSn (x = 1.3 *w*/%) alloy decreases with increasing Sn content, which is related to the volume fraction and distribution state of the second phase. In addition, Sn can also affect the stability of the oxide product film on the surface of magnesium alloy. According to the Mg-Sn binary phase diagram, the solid solubility of Sn in the Mg matrix ranges from 14.85 *w*/% at the eutectic temperature to 0.45 *w*/% at 200 °C when it is significantly decreased.[13] This indicates that Sn-containing second phases are easily formed in Mg alloys. The amount of Sn added should be limited to a relatively low level to avoid the formation of excessive Mg_2Sn phase. Metalnikov et al.[14] investigated the corrosion resistance of Mg-5Al-xSn alloy and found that the addition of Sn can form a dense oxide film containing SnO_2 on the surface of the alloy, improving its corrosion resistance. For Mg-Zn-Ca alloy, the mixing enthalpy of Sn-Ca is relatively negative (–45 kJ/mol).[15] The added elements easily combine with Ca to form CaMgSn,[8] thereby inhibiting the formation of Mg_2Sn phase.[16,17] In recent years, the microstructure evolution and mechanical properties of Mg-Zn-Ca alloys have been widely studied and reported.[18,19] Both Zn and Mg elements have a close-packed hexagonal structure (HCP). Therefore, the addition of Zn element has a strong effect on the solid solution strengthening and precipitation strengthening of magnesium alloys, and the addition of Zn element improves the tensile strength and elongation of an alloy. Ha[29] studied the effects of different Zn contents on the corrosion rate of Mg-5Sn alloy, and the results showed that Mg-5Sn-1Zn alloy had the best corrosion resistance. The addition of Zn had little effect on the grain size of the alloy. The hydrogen evolution rate and corrosion potential increased with the increase in the Zn content, and Zn dissolved in the α-Mg matrix had a protective effect on the oxide film. However, there is little research on the corrosion resistance of Mg-Zn-Ca alloy, especially the influence of CaMgSn on the corrosion behavior of the alloy. Therefore, in this study, 1 % Sn was added to Mg-6Zn-0.25Ca alloy to improve its corrosion resistance.

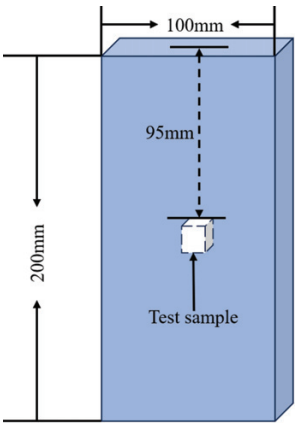

Figure 1: Sampling position of an alloy

2 EXPERIMENTAL PROCEDURE

In the experiment, industrial pure Mg (99.9 %), pure Sn (99.9 %), pure Zn (99.9 %) and Mg-25%Ca intermediate alloy were used to prepare 2kg of Mg-6Zn-0.25Ca and Mg-6Zn-1Sn-0.25Ca alloys. A type SG2-12-9 crucible resistance furnace was used for melting. The detailed process is as follows: Pure magnesium was put into the preheated crucible, and the crucible was heated to 750 °C. After the magnesium block was completely melted, the temperature was reduced to 710 °C; Mg-25%Ca alloy was added, followed by Sn block and Zn block successively after scraping, and stirred for 2–3 min. After 20 min, under the protection of a mixed gas (CO_2: SF_6 = 100:1), the melt was poured into a copper mold with a length of 100 mm, width of 25 mm and height of 215 mm. After cooling to room temperature, the board was homogenized (420 °C × 12 h). The chemical composition results for the alloy samples are shown in **Table 1**.

Firstly, the ingot head containing shrinkage defects (about 15 mm) was removed, then a wire cutting machine was used to take samples for an analysis. The sampling positions were all in the center of the plate, as

shown in **Figure 1**. A Shimazu 700 X-ray diffraction analyzer (XRD) was used to analyze the phase; a S4800 scanning electron microscope (SEM) was used to observe the phase morphology, and the element composition of the phase was detected with the attached energy dispersive spectrometer (EDS). Secondly, an immersion test was carried out as follows: a sample of (10 × 10 × 10) mm was immersed in an aqueous solution with a mass fraction of 3.5%NaCl for 24h; the precipitated hydrogen was collected by a burette, and the hydrogen evolution data was recorded every 2 h. In order to keep the concentration of the solution stable, the NaCl solution was replaced every 12 h. After the corrosion, the sample was taken out and placed into the prepared chromate solution, then cleaned with ultrasonic waves for 10 min.

Table 1: Chemical compositions of the magnesium alloys (φ/%)

Alloy	Zn	Ca	Sn	Mg
Mg-6Zn-0.25Ca	5.95	0.244	0.994	Bal.
Mg-6Zn-1Sn-0.25Ca	5.73	0.246	-	Bal.

The weight loss rate is calculated using the following Equation:[28]

$$P_w = \frac{8.76 \cdot 10^4 \cdot \Delta g}{A \cdot t \cdot \rho}$$

The hydrogen evolution rate is calculated using the following Equation:[28]

$$P_H = \frac{8.76 \cdot 10^4 \cdot \Delta V \cdot M}{A \cdot t \cdot \rho}$$

Here: P_W – the weight loss rate, mm·a^{-1}; Δg – the mass loss before and after alloy corrosion, g; ΔV – the total amount of hydrogen precipitated during corrosion, mL; M – the relationship between the hydrogen production rate and the alloy mass loss rate, the value is 0.001083 g·mL^{-1}; A – the total surface area of a soaked specimen, cm^2; t – the soaking time, h; ρ – the weight loss measurement sample density, g·cm^{-3}. The polarization curve and impedance of the alloy were measured using a CHI660E electrochemical workstation. The saturated calomel electrode was used as the reference electrode; the platinum electrode was the auxiliary electrode, and the sample was the working electrode.

3 RESULTS AND DISCUSSION

3.1 Microstructure analysis

Figure 2 shows the XRD patterns of ZX60 and ZXT601 alloys. It can be seen that ZX60 alloy is composed of two phases, including α-Mg and $MgZn_2$. ZXT601 alloy is composed of three phases, including α-Mg, CaMgSn and $MgZn_2$. In ZX60 alloy, the Ca element does not form a new phase with the other elements, but dissolves in the magnesium matrix, distributing uniformly in the alloy. The addition of the Sn element also

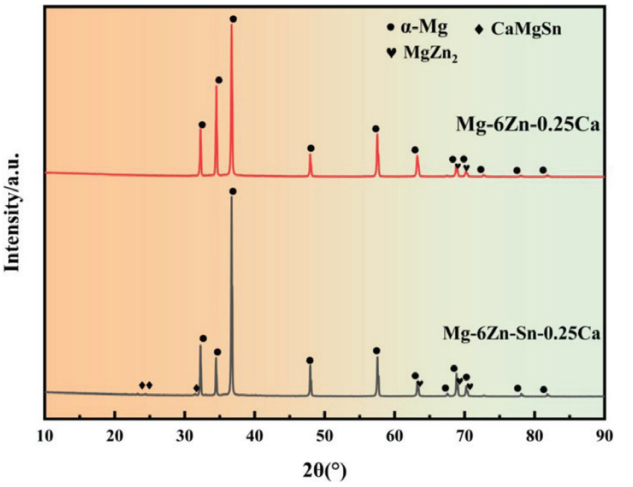

Figure 2: XRD patterns of homogeneous ZX60 and ZXT601 alloy

promotes the precipitation of $MgZn_2$ phase. In addition, according to the literature, the formation of CaMgSn phase is mainly related to the mass ratio of Sn/Ca. When the mass ratio of Sn/Ca in ZXT601 alloy is close to 3, CaMgSn is the predominant phase in the alloy.[20]

To further qualitatively and quantitatively analyze the composition, morphology and distribution of the second phase in the as-cast structure of the alloy, the alloy was analyzed with the scanning electron microscope (SEM). **Figure 3** shows the microstructure and phase distribution of the homogenized alloy. The average grain size of ZX60 alloy is 144 μm; it includes a small amount of a point-like second phase. After the addition of 1 % Sn, the grain size is reduced to 64 μm, and a large number of point-like and strip-like second phases are precipitated. The corresponding energy dispersive analysis (EDS) results are shown in **Table 2**. Although a small amount of Ca is detected in ZX60 alloy, Mg_2Ca phase is formed in the Mg-Zn-Ca system when the Zn/Ca atomic ratio is less than 1.2. In this experiment, the Zn/Ca atomic ratio is greater than 1.2. Based on this atomic ratio and the XRD results, it is inferred that there is no Mg_2Ca phase. In addition, $MgZn_2$ exists in two forms: strip-like and point-like. The addition of Sn reduces the volume of the second phase, forming point-like and strip-like CaMgSn phases. It can be seen from the metallographic diagram that there are relatively obvious grain boundaries, but with the addition of Sn, the grain boundaries disappear and are replaced by a point-like second phase.

Table 2: EDS analysis of the precipitated phases of the two alloys

Point	Chemical composition (φ/%)				Phase types
	Mg	Zn	Ca	Sn	
A	79.34	2.89	4.83	12.94	CaMgSn
B	71.16	3.08	10.14	15.61	CaMgSn
C	52.45	38.95	8.61		$MgZn_2$
D	59.18	32.23	8.58		$MgZn_2$

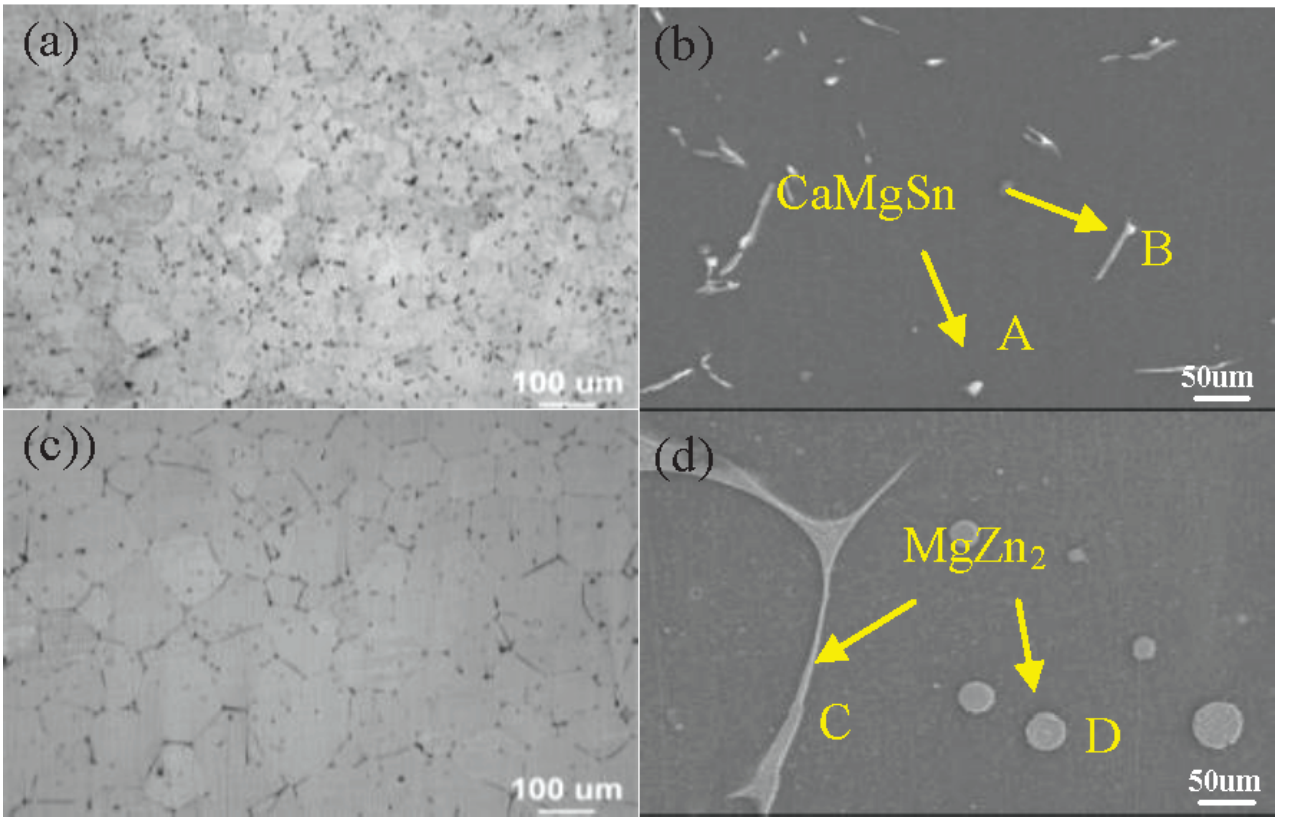

Figure 3: Microstructure and EDS analysis of ZX60 (a, b) and ZXT601(c, d) homogeneous alloys

3.2 Corrosion resistance

Figure 4 shows macroscopic and SEM images of the two alloys after soaking for 24h. Comparing **Figures 4a** and **4b**, it is found that the surface corrosion of ZX60 alloy is relatively serious, and the corrosion pit after the spalling of corrosion products can be clearly seen. This was mainly caused by the corrosion dissolution of α-Mg. Compared with ZX60 alloy, the surface corrosion of ZXT601 alloy is smaller; there is no obvious corrosion pitting, and a slight metal luster can be observed on its

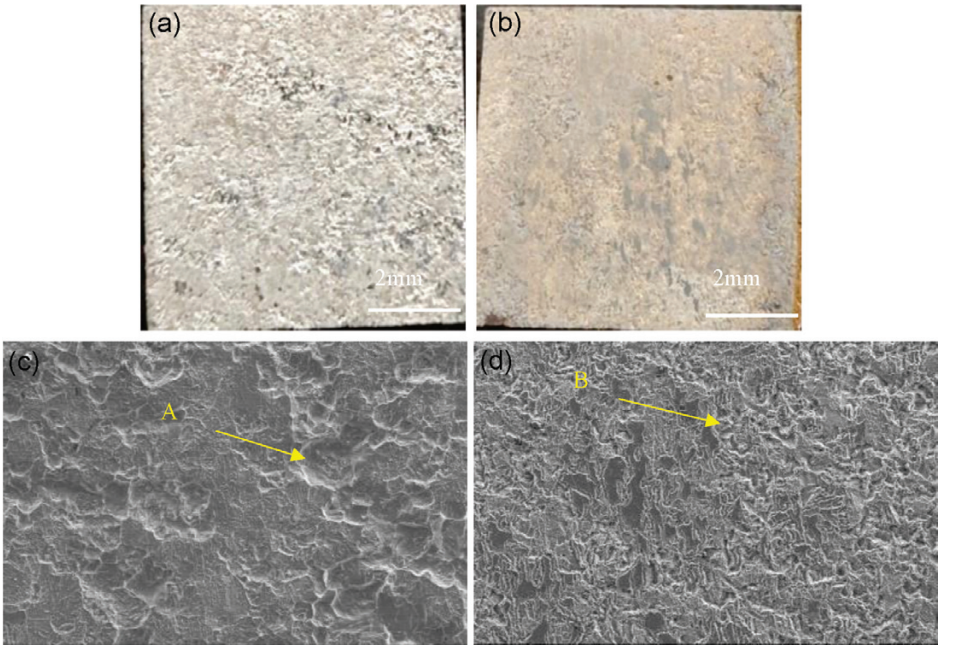

Figure 4: Macroscopic and SEM images of homogenized ZX60 (a, c) and ZXT601 (b, d) alloys

surface. As can be seen from the SEM photos in **Figures 4c** and **4d**, the corrosion pits (spot A) of ZX60 alloy are deeper than the corrosion pits (spot B) of ZXT601 alloy. This shows that the corrosion of ZX60 alloy is more serious, and the corrosion of ZXT601 alloy is shallow. The analysis suggests that this is because the addition of Sn makes the corrosion product film formed on the surface of ZXT601 alloy denser, which effectively protects the matrix.

The changes in the hydrogen volume and average corrosion rate of ZX60 and ZXT601 alloys soaked for 24 h are shown in **Figure 5**. Here, we see a linear relationship between the amount of hydrogen precipitated and the soaking time, indicating that the amounts of hydrogen produced in both periods are almost equal. It is also clear that the amount of hydrogen precipitated by ZX60 alloy is much higher than that of ZXT601 alloy, indicating that its corrosion resistance is relatively poor. The hydrogen evolution rate of magnesium dissolution should be equal to the weight loss rate,[21] but it is found from the figure that the weight loss corrosion rate of the two alloys is slightly higher than the hydrogen evolution corrosion rate. It is established that a very small amount of hydrogen escapes during hydrogen evolution corrosion, and it does not affect the test results. It can be concluded from the immersion test that the corrosion resistance of ZXT601 alloy is good, that is, adding 1 % Sn can reduce the corrosion rate of ZX60 alloy.

Figure 6 shows the polarization curves and Nyquist diagrams of ZX60 and ZXT601 alloys. In general, the cathode polarization curve represents the hydrogen evolution reaction due to water reduction, while the anode polarization curve represents the dissolution of the magnesium matrix. It can be seen from the polarization curves that the corrosion potentials and corrosion currents of the two alloys are very different. It has been pointed out that factors affecting the electrochemical reactions of alloys include thermodynamic factors and dynamic factors of alloys. Studies have shown[22] that the self-corrosion potential of alloys affects the corrosion resistance of alloys, and the self-corrosion potential of alloys refers to the stable potential under the condition without external polarization. The higher the self-corrosion potential, the less likely the alloy is to corrode. However, the final corrosion behavior of the alloy is still determined by the dynamic factor of the alloy, that is, the size of the alloy's self-corrosion current density (I_{CORR}). Therefore, the corrosion current density of ZX60 alloy is much higher than that of ZXT601 alloy, indicating that the corrosion resistance of ZXT601 alloy is better than

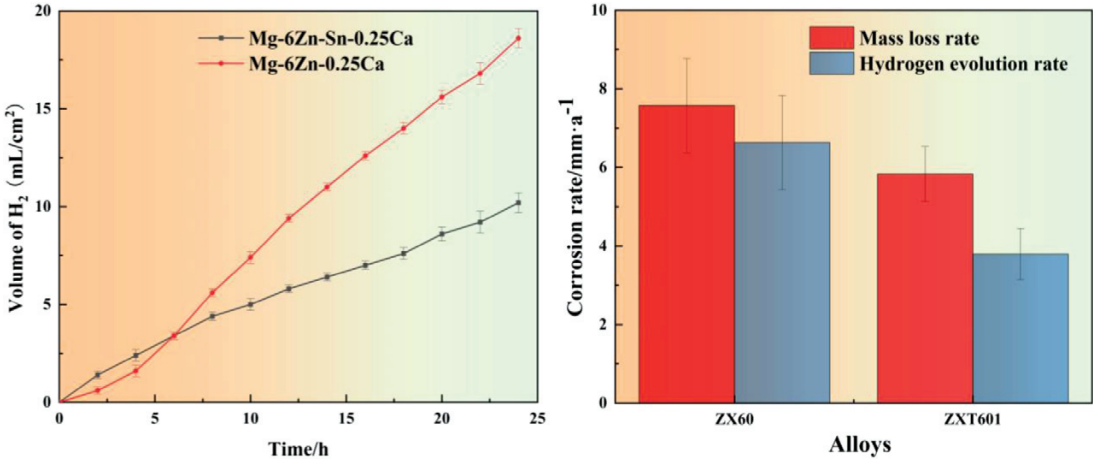

Figure 5: Corrosion of homogenized ZX60 and ZXT601 alloys immersed for 24 h: a) hydrogen content and b) corrosion rate

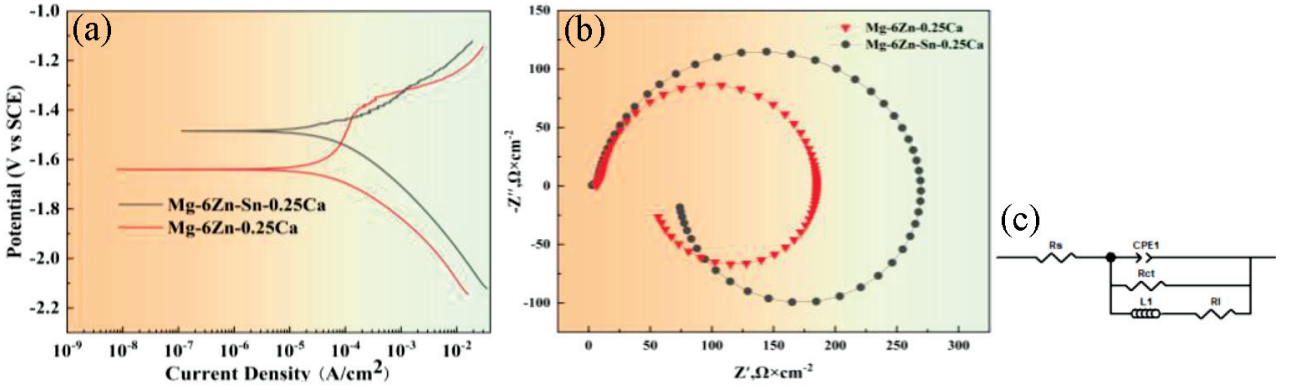

Figure 6: a) Polarization curves, b) Nyquist diagrams, and c) fitting circuits of homogenized X60 and ZXT601 alloys

that of ZX60 alloy. The polarization curve is consistent with the soaking test results. Generally speaking, the polarization curve reflects the thermodynamic tendency of corrosion, and electrochemical impedance spectroscopy (EIS) result reflects the dynamic tendency of corrosion. EIS is usually used to determine the actual corrosion resistance of a material, while the polarization curve serves as a complementary technique.[27]

Therefore, to further study the corrosion mechanism of the two alloys, the impedance spectra of the two alloys are represented by the Nyquist curves, as shown in **Figure 6b**. The Nyquist curves of both ZX60 and ZXT601 alloys have one high frequency capacitive reactance arc and one low frequency inductive reactance arc, indicating that the addition of Sn does not change the corrosion mechanism. Of the two, ZXT601 alloy exhibits the largest arc resistance at any frequency, indicating that its surface charge transfer resistance and surface film resistance are the highest. The oxidation product film exhibits good stability during dynamic corrosion, and can hinder the corrosion of α-Mg matrix to a certain extent, indicating that its corrosion resistance is the best.[28] Equivalent circuit fitting was performed on the impedance spectra of ZX60 and ZXT601 alloys (as shown in **Figure 6c**), and the specific parameters are shown in **Table 3**. Among them, R_s is the solution resistance, R_t is the corrosion product film resistance, R and L in series indicate pitted areas on the surface of the alloy, and the constant phase element (CPE_{dl}) is used in parallel with the resistance (R_{ct}) to fit the high frequency capacitor-reactance arc in the equivalent circuit. R_L is the charge transfer resistance, and the larger the value, the smaller the electrochemical rate and the slower the corrosion rate. R_t is the corrosion product film resistance, and the higher the value, the more corrosion resistant the corrosion film. In **Table 3**, R_L(ZXT601)>R_L(ZX60), R_t(ZXT601)>R_t(ZX60). Therefore, it can be concluded that both ZX60 and ZXT601 alloys have pitting corrosion on the surface during corrosion, but the product film destruction rate and pitting expansion of ZXT601 alloy are smaller than those of ZX60 alloy. The results are consistent with the above conclusions, that is, the corrosion resistance of ZXT601 alloy is better than that of ZX60 alloy. In summary, the weight loss and hydrogen evolution tests show that the corrosion rate of ZXT601 alloy is lower than that of ZX60 alloy.

As can be seen from the Tafel polarization curve, asymmetrical anode and cathode branches appear in both alloys. It is worth noting that the cathode curve of ZX60 alloy includes an obvious passivation zone, indicating that after the alloy pitting, there is a corrosion film. However, its existence is not stable, it cannot effectively protect the magnesium matrix, resulting in poor corrosion resistance of the alloy. In ZXT601 alloy, the self-corrosion potential is higher, but the self-corrosion current density is lower, and a weak passivation zone can be observed on the cathode curve of the alloy. This indicates that the corrosion tendency of ZXT601 alloy is higher, but the corrosion film formed on the surface is more stable than that of ZX60 alloy, reducing the formation of corrosion pits, as shown in **Figure 4**.

Table 3: Corrosion potential and corrosion current density of homogenized ZX60 and ZXT601 alloys in 3.5 % NaCl solution

Alloy	E_{corr}/V	I_{corr}/μA·cm^2	P_i/(mm/a)
Mg-6Zn-Sn-0.25Ca	–1.483	22.03	5.03
Mg-6Zn-0.25Ca	–1.637	29.86	6.82

It has been pointed out that the precipitation of $MgZn_2$ phase correspondingly reduces the corrosion resistance of magnesium alloy, but the corrosion products formed have good corrosion resistance, and the adhesion to the surface of the matrix prevents a further reaction of the matrix. In addition, the corrosion resistance of magnesium alloy is the result of the joint action of grain size, microstructure uniformity and defect density.[23] Some studies[24,25] showed that a smaller grain size can improve the corrosion resistance of magnesium alloys, while the second phase in the alloy also plays a crucial role in the corrosion behavior of magnesium alloys. When a magnesium alloy is immersed in a 3.5%NaCl solution, the second phase usually acts as a micro cathode, and galvanic corrosion occurs between the magnesium matrix and the second phase, resulting in rapid corrosion of the magnesium matrix around the second phase.[26] If the volume fraction of the second phase is higher and the distribution is more uniform, a denser and more compact corrosion film is formed on the magnesium matrix, which acts as a barrier preventing corrosion. Otherwise, the corrosion film is loose and accelerates the corrosion of the alloy. In this study, the addition of Sn significantly improves the corrosion resistance of ZX60 alloy, and its mechanism is shown in **Figure 7**. Firstly, the addition of Sn significantly refines the grain size of ZX60 alloy, inhibits the hydrogen evolution reaction at the cathode, and thus impedes the dissolution of the anode. In addition, compared with ZX60 alloy with more severe local corrosion (**Figure 4a**), ZXT601 alloy exhibits a denser distribution of CaMgSn phase and an increased precipitation of $MgZn_2$ phase. Therefore, the passivation film formed during the

Table 4: Equivalent circuit fitting results for ZX60 and ZXT601 alloys

Alloy	R_s	CPE_{dl}	R_T	R_L	L	
	Ω·cm^2	Y_1/μΩ^{-1}·cm^{-2}	n_1	Ω·cm^2	Ω·cm^2	H·cm^2
Mg-6Zn-0.25Ca	6.955	3.074·10^{-5}	0.90	183.2	60.36	755.5
Mg-6Zn-1Sn-0.25Ca	5.033	4.554·10^{-5}	0.841	274.7	70.6	216.1

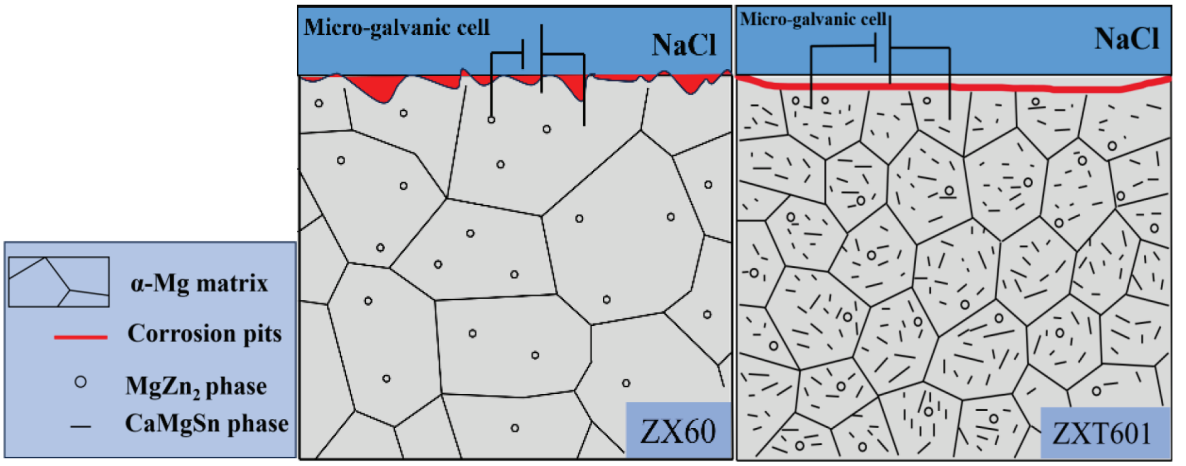

Figure 7: Corrosion mechanism of homogenized ZX60 and ZXT601 alloys

corrosion is more uniform, Sn-based corrosion products are more resistant than the Mg matrix, and the corrosion products cover the alloy surface without defects, reducing the corrosion rate (**Figure 4b**). In addition, compared with ZX60 alloy, the precipitation of $MgZn_2$ phase can be promoted by Sn. It is beneficial to improving the corrosion resistance of ZXT601 alloy. Therefore, the corrosion resistance of ZXT601 alloy is improved under a joint action of uniformly distributed CaMgSn phase and $MgZn_2$ phase.

4 CONCLUSION

1) The addition of the Sn element refined the grain size of the homogenized ZX60 alloy and made ZXT601 alloy have a more uniform distribution of CaMgSn phase. It also increased the precipitation of $MgZn_2$ phase. However, Sn did not form a second phase with the other alloy elements, but was uniformly distributed in the α-Mg matrix.

2) The addition of the Sn element effectively reduces the corrosion rate of ZX60 alloy, which is mainly associated with the refinement of alloy grains and a more uniform distribution of CaMgSn second phase.

3) EIS results indicate that the Nyquist curves of ZX60 and ZXT601 alloys consist of one capacitance arc in the high-frequency region and one inductance arc in the low-frequency region, indicating that the corrosion mechanisms of the two alloys are the same. However, from the diameter of the Nyquist curve, it can be concluded that ZXT601 has better corrosion resistance than ZX60 alloy.

Acknowledgements

The authors acknowledge the financial support from the Liaoning Province Natural Science Foundation Project of China (2023-MS-321) and the Liaoning Province International Cooperation Project (Project Number: 2023030491-JH2/107).

5 REFERENCE

[1] K. Hono, C. L. Mendis, T. T. Sasaki et al., Towards the development of heat treatable high-strength wrought Mg alloys, Scr. Mater., 63 (**2010**), 710–715

[2] Z. R. Zeng, Y. M. Zhu, M. Z. Bian et al., Annealing strengthening in a dilute Mg–Zn–Ca sheet alloy, Scr. Mater., 107 (**2015**), 127–130

[3] T. Tu, X.-H. Chen, J. Chen et al., A High-Ductility Mg–Zn–Ca Magnesium Alloy, Acta Metall. Sin.-Engl., 32 (**2019**), 23–30

[4] M. Esmaily, J. E. Svensson, S. Fajardo et al., Fundamentals and advances in magnesium alloy corrosion, Prog. Mater. Sci., 89 (**2017**), 92–193

[5] A. Atrens, Z. M. Shi, S. U. Mehreen et al., Review of Mg alloy corrosion rates, J. Magnes. Alloy., 8 (**2020**), 989–998

[6] Y. S. Jeong, W. J. Kim, Enhancement of mechanical properties and corrosion resistance of Mg-Ca alloys through microstructural refinement by indirect extrusion, Corrosion Science, 82 (**2014**), 392–403

[7] Y. M. Jin, C. Blawert, F. Feyerabend et al., Time-sequential corrosion behavior observation of micro-alloyed Mg-0.5Zn-0.2Ca alloy via a quasi-in situ approach, Corrosion Science, 158 (2019)

[8] S. G. Bratsch, Standard Electrode Potentials and Temperature Coefficients in Water at 298.15 K, J. Phys. Chem. Ref. Data, 18 (**1989**), 1–21

[9] Hucheng Pan, Gaowu Qin, Ming Xu et al., Enhancing mechanical properties of Mg–Sn alloys by combining addition of Ca and Zn. Materials & Design, 83 (**2015**), 736

[10] K. Suresh, K. P. Rao, Y. V. Prasad et al., Microstructure and mechanical properties of as-cast Mg-Sn-Ca alloys and effect of alloying elements, Transactions of Nonferrous Metals Society of China, 23 (**2013**) 12, 3604–3610

[11] Boby Arun, A. Srinivasan, U. T. S. Pillai et al., Mechanical characterization and corrosion behavior of newly designed Sn and Y added AZ91 alloy, Materials & Design, 88 (**2015**), 871

[12] C. Zhao, F. Pan, S. Zhao et al., Microstructure, corrosion behavior and cytotoxicity of biodegradable Mg–Sn implant alloys prepared by sub-rapid solidification, Mater. Sci. Eng. C, 54 (**2015**), 245–251

[13] S. Wei, T. Zhu, M. Hodgson et al., Effects of Sn addition on the microstructure and mechanical properties of as-cast, rolled and annealed Mg–4Zn alloys, Mater. Sci. Eng. A, 585 (**2013**), 139–148

[14] P. Metalnikov, G. Ben-Hamu, D. Eliezer et al., Role of Sn in microstructure and corrosion behavior of new wrought Mg-5Al alloy, J. Alloys Compd., 777 (**2019**), 835–849

[15] A. Takeuchi, A. Inoue, Classification of bulk metallic glasses by atomic size difference, heat of mixing and period of constituent elements and its application to characterization of the main alloying element, Mater. Trans., 46 (**2005**), 2817–2829

[16] C. Wang, Z. Liu, S. Xiao et al., Effects of Sn, Ca additions on thermal conductivity of Mg matrix alloys, Mater. Sci. Technol., 32 (**2016**), 581–587

[17] A. Kozlov, M. Ohno, R. Arroyave et al., Phase equilibria, thermodynamics and solidification microstructures of Mg–Sn–Ca alloys, Part 1: Experimental investigation and thermodynamic modeling of the ternary Mg–Sn–Ca system, Intermetallics, 16 (**2008**), 299–315

[18] H. C. Pan, G. W. Qin, Y. M. Huang et al., Development of low-alloyed and rare-earth-free magnesium alloys having ultra-high strength, Acta Mater., 149 (**2018**), 350–363

[19] A. Zhang, R. Kang, L. Wu et al., A new rare-earth-free Mg-Sn-Ca-Mn wrought alloy with ultra-high strength and good ductility, Mater. Sci. Eng. A, 754 (**2019**), 269–274

[20] C. Wang, S. Guo, L. Zeng et al., Effects of second phases on microstructure, microhardness, and corrosion behavior of Mg-3Sn-(1Ca) alloys, Materials (Basel), 12 (**2019**) 16, 2515

[21] Changwei Gong, Xinze He, Xue Yan, Corrosion behavior of Mg–Ca–Zn alloys with high Zn content, Journal of Physics and Chemistry of Solids, 152 (**2021**) 1

[22] Xuejian Wang, Study on corrosion behavior of Mg-5Sn(-In-Ga) alloys, Dalian University of Technology, 2022

[23] Tong Hu, Wenlong Xiao, Fang Wang et al., Improving tensile properties of Mg-Sn-Zn magnesium alloy sheets using pre-tension and ageing treatment, Journal of Alloys and Compounds,735 (**2018**), 1494

[24] Pingli Jiang, Carsten Blawert, Jan Bohlen et al., Corrosion performance, corrosion fatigue behavior and mechanical integrity of an extruded Mg4Zn0.2Sn alloy, Journal of Materials Science & Technology, 59 (**2020**), 107

[25] Pingli Jiang, Carsten Blawert, Nico Scharnagl et al., Mechanistic understanding of the corrosion behavior of Mg4Zn0.2Sn alloys: From the perspective view of microstructure, Corrosion Science, 174 (**2020**), 108863

[26] Soomin Baek, Jeongsu Kang, Jongchan Kim et al., Corrosion Science, 141 (**2018**), 203

[27] Jaeho Kwon, Soomin Baek, Hoseok Jung et al., Role of micro alloyed Sm in enhancing the corrosion resistance of hot-rolled Mg-8Sn-1Al-1Zn alloy, Corrosion Science, 185 (**2021**), 109425

[28] Siqi Yin, Wenchao Duan, Wenhong Liu et al., Influence of specific second phases on corrosion behaviors of Mg-Zn-Gd-Zr alloys, Corrosion Science, 166 (**2020**), 108419

[29] S. Lesz, B. Hrapkowicz, M. Karolus, et al., Characteristics of the Mg-Zn-Ca-Gd alloy after mechanical alloying, Materials, 14 (**2021**) 1, 226